Improved Speed and Sensitivity in RNA Covariance Model Searches

Eric P. Nawrocki and Sean R. Eddy
Howard Hughes Medical Institute & Department of Genetics,
Washington University School of Medicine
Saint Louis, Missouri 63110 USA
eddy@genetics.wustl.edu

April 19, 2006

Abstract

Background: Covariance models (CMs) are probabilistic models of RNA secondary structure; a special case of profile stochastic context-free grammars (profile SCFGs), analogous to profile hidden Markov models of linear sequence. The dynamic programming algorithm for searching a database of L residues with a query RNA structure of N residues is $O(N^3L)$. Poor search speed is a major factor limiting practical applications of CM methods.

Methodology/Principal Findings: To accelerate CM database search, we describe a method for precalculating probabilistic bounds on which cells of the CYK dynamic programming matrix need to be calculated. These bounds are calculated *a priori*, independent of the target database sequence. We also describe the estimation of emission and transition prior probabilities and an entropy weighting strategy that make CMs more sensitive for homology detection. A new release of the INFERNAL software package, version 0.70, which implements the techniques and algorithms discussed here, is now freely available from our lab's website.

Conclusions/Significance: Preliminary results on an Rfam based benchmark show that CMs are now significantly more sensitive and a speed-up of 3-5X on average is achievable with the banded CYK algorithm, without an appreciable cost in performance.

Introduction

Non-coding RNA (ncRNA) genes encode functional RNA molecules that are not translated to proteins. Our understanding of the importance and breadth of the roles of ncRNAs in the cell continues to grow through both discovery of novel families and further study of known families, including comparative sequence analysis of homologs across species. But ncRNA genes are difficult to find relative to protein coding genes. Their small size and immunity to frameshift mutations make them hard to detect by mutational genetic screens, and they do not lie within open reading frames hiding them from traditional computational gene-finders. However, many RNA families exhibit conservation at the structural and sequence level, and computational analyses that consider both of these types of information have been informative. These efforts have mainly focused on three fundamental problems: finding novel RNAs, folding RNAs of unknown structure, and finding homologous RNAs.

Of current interest is the third problem: RNA homology detection in genomic sequence. Given a consensus structure and known members of a family, we want to be able to find more. There are two main classes of existing homology detection tools. The first class is specific to a certain family or motif. For example, specialized programs exist to search for tRNAs [1], snoRNAs [2], microRNAs [3,4], SRP RNAs [5], and rho-independent transcription terminators [6], among others. By definition, these approaches are not generalizable, and were built using expert knowledge of the family being modeled. In contrast, the second class of tools are general, designed to work for any family. These include pattern description methods [7,8], as well as probabilistic models called profile stochastic context-free grammars (SCFGs) [9, 10].

Profile SCFGs are generalizations of profile HMMs, with added complexity necessary for modelling base-pairing interactions. These models are formally grounded in probability theory, and dynamic programming (DP) algorithms exist to search for and align homologous RNA sequences [11]. But these methods are computationally expensive, and the main impediment to their potential routine use is the $O(N^3 logN)$ time complexity of the DP algorithms and its implications; most seriously the impracticality of genomic searches.

Here we focus on a particular formulation of profile SCFGs called “covariance models” (CMs) [9, 11, 12]. Relative to profile HMM methods, CM methods are still in their infancy, and several general techniques that have increased the sensitivity of profile HMMs, such as informative prior distributions for parameter estimation [13], have not yet been applied to CMs. Despite this, CMs are used by the Rfam database [14] to annotate ncRNAs in complete genomes. Rfam version 7.0 includes 503 RNA families, each represented by a CM built from a manually constructed, consensus structure annotated input alignment that. The CM is used to classify and align new family members in a genomic database. Because CM searches are so slow (searching the 3 GB human genome for RNase P on a single processor would take roughly 15 years), during annotation the Rfam curators first use BLAST to filter the database, and use the CM to search only the surviving fraction that has scored above a threshold.

While fast, the BLAST step may miss some homologs a full CM based search would have found. This issue has been addressed nicely by Zasha Weinberg and Larry Ruzzo through development of two profile HMM based filtering methods to replace BLAST. Given a CM, their first strategy builds a *rigorous filter* HMM, that is guaranteed to allow every hit that would score above a given threshold to the CM to survive the filtering step [15,16]. The second strategy builds a *maximum likelihood (ML) heuristic* HMM from a CM that is not rigorous but more practical to use as a filter for many RNA families [17]. For current Rfam models, these new filters offer roughly a 100 fold speed up relative to a full CM based search at either no cost (with rigorous filters), or a small cost (with ML HMMs) to sensitivity.

A limitation of all three of these filtering methods is their dependence on primary sequence conservation, which makes them less effective for RNA families that exhibit stronger structural than sequence conservation. In general, the less sequence conservation in a family, the smaller the database fraction that can be removed by a primary sequence based filter. Although many current Rfam families exhibit relatively high sequence conservation, this is likely due, at least in part, to ascertainment bias because many Rfam homologs were detected using BLAST or other primary sequence based methods. As detection tools become more sensitive and more distant homologs are discovered, we expect the observed sequence identity within many of these families to decrease, making filters less useful. In practice, for many current Rfam families with low sequence identity the CM based search of the filtered fraction (determined using any filtering technique) takes longer than the filtering step [17]. This suggests that an accelerated CM search algorithm would be useful to complement filtering. Here, we present a method for accelerating CM searches that is based on the concept of banded alignment.

A banded alignment approach aims to save time by ignoring potential alignments that are unlikely to be high scoring or optimal. In the context of dynamic programming (DP), bands (sometimes called constraints) designate boundaries on which cells of the DP matrix should be considered during alignment; cells outside the bands are ignored. Importantly, imposing bands sacrifices the guarantee that the optimal DP solution will be found, but in practice the approach is useful if appropriate bands are defined.

There are many examples of banded alignment in sequence analysis programs. For instance, LAGAN and MULTI-LAGAN use banded dynamic programming (referred to as limited-area dynamic programming) to stitch together alignments between anchored sequences when aligning long, genomic sequences. BLAST uses a related technique to decide when to stop extending high-scoring segment pairs (HSPs) [18]. The simultaneous RNA alignment and structure prediction programs CONSAN [**?**], DYNALIGN [19], and STEMLOC [20] each use a different banding strategy to limit the time complexity of variants of the Sankoff algorithm [21]. Banding has also been applied to profile SCFGs by Michael

Brown in his RNACAD program by using information from a profile HMM alignment to define bands for the expensive SCFG alignment [22].

Here, we present a novel method to accelerate CM database search using probabilistically determined bands calculated independently of the target database. We also describe the extension to CMs of several techniques borrowed from the profile HMM community: informative transition priors, which enable appropriate band calculation, along with informative emission priors and model entropy weighting to increase CM sensitivity . Finally, to measure the effect of these techniques, and the utility of our banded approach, we present the results of an Rfam based benchmark.

Results

A CM database search for RNA homologs finds subsequences of the database that align with a high score to the model. The key idea of our technique for acceleration is to save time by ignoring highly unlikely alignments using bands that restrict the possible subsequence lengths that can be aligned to each part of the model. We present a method for calculating and enforcing these bands that is independent of the database, and show that our method accelerates CM methods with a small cost to accuracy.

Covariance models

Covariance models (CMs) are probabilistic models of the consensus secondary structure and sequence of a family of non-coding RNAs. CMs are organized in a tree-like, directed graph of states. The first state is the root of the tree and is customarily drawn at the top. The states are conceptually organized into different types of nodes, with characteristic sets of states within each node type. The organization of the nodes is defined by the consensus structure of the RNA family being modeled, which must be definedp prior to CM construction [12, 23].

CMs can be thought of as generative models that *emit* RNA sequences. A new sequence is emitted by starting at the leaves of the tree and moving upwards from state to state following specific *production rules* and emitting residues on both the left and right sides of the growing sequence. When a bifurcation state is reached, a split of the sequence is created, and the sequence continues to grow in both directions on each side of the split. Only specific transitions from state to state are allowed, namely a state v can only transit to its children states y in the set C_v. For each production rule, probabilities are associated with each possible residue emission ($e_v(a)$) and transition ($t_v(Y)$) [9]. We refer to the number of residues emitted by each state v on the left and right as Δ_v^L and Δ_v^R, respectively. A CM consists of states of seven different types, each with a corresponding production rule:

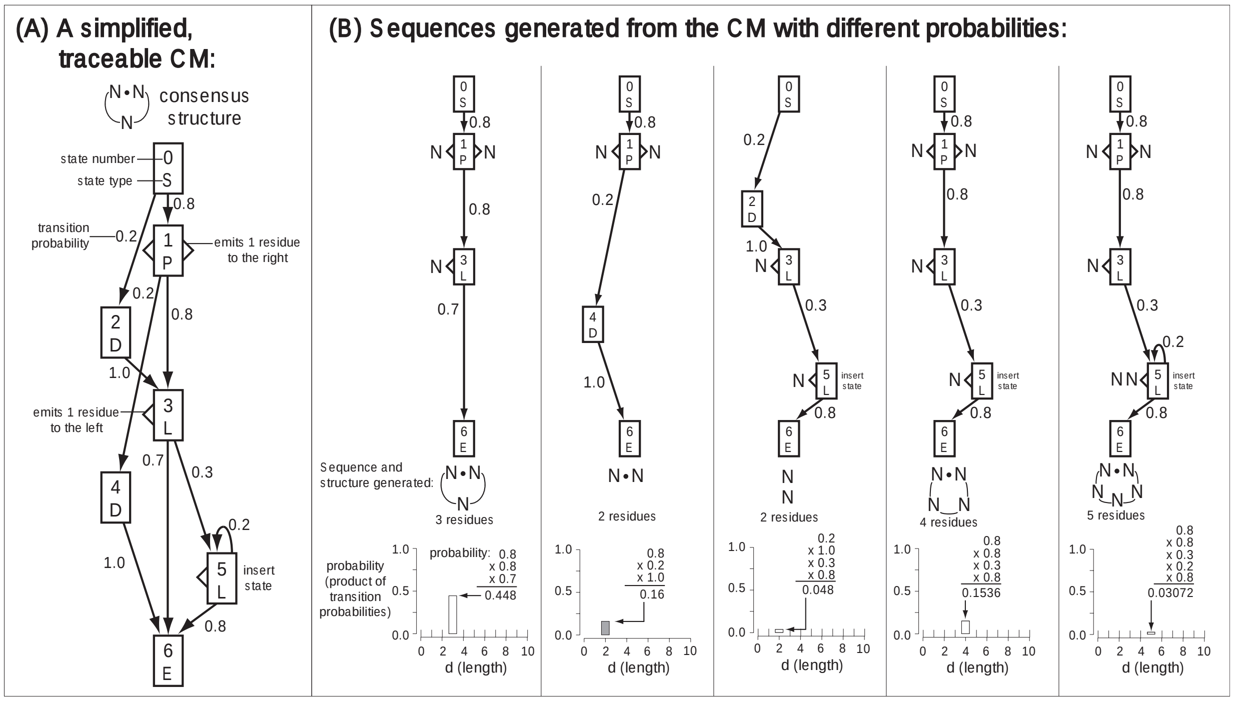
(A) A simplified, traceable CM:
N•N N consensus structure
state number
state type
transition probability
emits 1 residue to the right
emits 1 residue to the left
insert state
0 S
1 P
2 D
3 L
4 D
5 L
6 E
0.8
0.2
1.0
0.7
0.3
(B) Sequences generated from the CM with different probabilities:
Sequence and structure generated:
3 residues
2 residues
4 residues
5 residues
probability (product of transition probabilities)
probability: 0.8 x 0.8 x 0.7 0.448
0.8 x 0.2 x 1.0 0.16
0.2 x 1.0 x 0.3 x 0.8 0.048
0.8 x 0.8 x 0.3 x 0.8 0.1536
0.8 x 0.8 x 0.3 x 0.2 x 0.8 0.03072
d (length)

Figure 1: **A simplified CM. (A):** Biologically unrealistic, toy CM with simplified architecture. **(B):** Examples of sequences generated from CM in (A), each with its own probability given the transition probabilities of the model, as shown in plots at bottom.

State type	Description	Production	Δ_v^L	Δ_v^R	Emission	Transition
P	(pair emitting)	$P \rightarrow aYb$	1	1	$e_v(a,b)$	$t_v(Y)$
L	(left emitting)	$L \rightarrow aY$	1	0	$e_v(a)$	$t_v(Y)$
R	(right emitting)	$R \rightarrow Ya$	0	1	$e_v(a)$	$t_v(Y)$
B	(bifurcation)	$B \rightarrow SS$	0	0	1	1
D	(delete)	$D \rightarrow Y$	0	0	1	$t_v(Y)$
S	(start)	$S \rightarrow Y$	0	0	1	$t_v(Y)$
E	(end)	$E \rightarrow \epsilon$	0	0	1	1

A simplified CM with examples of emitted sequences is shown in Figure 1.

Although it is convenient to think of CMs as generative models, their utility lies in the ability to align existing sequences and score the alignments to predict homology. Given a parameterized model and a sequence, the CYK dynamic programming algorithm optimally aligns the sequence to the model by determining the most probable path through the model that could have generated the sequence [11]. The algorithm is easily extended to allow local alignment to the model by permitting transitions that bypass subtree(s) of the model [24].

Accelerating CM methods using a banded strategy

The banded method we introduce accelerates CYK alignment by reducing the number of potential paths through the model that are considered. This technique relies on two specific features of the SCFG architecture of CMs. Notably, this approach is applicable to any probabilistic model with the following two characteristics, however we believe it is mainly useful for SCFG methods:

1. Cycles in the graph (tree) of states are restricted to emitting rules.

2. With states numbered in preorder traversal, no state v can transit to a state y if $v > y$.

The alignment of a sequence to a CM is represented as a *parse tree* which specifies the boundaries of the subsequences that are aligned to each subtree of the model. The CYK algorithm determines the most likely parse tree of a sequence given a CM by considering the alignment of all possible length subsequences (from 0 up to L, the length of the RNA) to each subtree. Our banded strategy determines and enforces state specific bounds on the lengths of subsequences that are permitted to be aligned to each subtree of the model (each state is the root of a different subtree). The bounds are implemented as bands on the CYK dynamic programming matrix; cells outside the bands are ignored. Next, considering the CM as a generative model, we present an algorithm that determines these bands from the transition probabilities of the model.

Band calculation algorithm

The band calculation algorithm iteratively calculates $\gamma_v(d)$, the probability that the subtree of the model rooted at state v will generate a subsequence of length d. This is the summed probability of all possible paths through the subtree rooted at v (i.e. paths that start at v and end at the nearest E state $y > v$) that emit exactly d residues. The calculation initializes at the smallest subtrees (E states) and shortest subsequences ($d = 0$) and iterates upwards and outwards to progressively larger subtrees and longer subsequences. The band calculation algorithm is as follows:

for $v = M$ down to 1:

$v =$ end state (E):	$\gamma_v(0) = 1$	
	$\gamma_v(d) = 0$	for $d = 1$ to Z
$v =$ bifurcation (B):	$\gamma_v(d) = \sum_{n=0}^{d} \gamma_y(n) * \gamma_z(d-n)$	for $d = 0$ to Z
else ($v = S, P, L, R$):	$\gamma_v(d) = 0$	for $d = 0$ to $(\Delta_v^L + \Delta_v^R - 1)$
	$\gamma_v(d) = \sum_{y \in C_v} \gamma_y(d - (\Delta_v^L + \Delta_v^R)) * t_v(y)$	for $d = (\Delta_v^L + \Delta_v^R)$ to Z

For example, if we're calculating $\gamma_v(d)$ and v is is a pair state we know that state v will emit a pair of residues and transit to a new state y (one of its possible transitions C_v) which then will have to account for the smaller subsequence of length $d-2$. Therefore, $\gamma_v(d)$ is the sum, over all possible states y in C_v, of the probability of transiting to y $(t_v(y))$ and generating a subsequence of length $(d-2)$ from the subtree rooted at y (i.e. the previously calculated solution $\gamma_y(d-2)$). For B states, the algorithm uses γ values for predefined children states y and z. Figure 2 traces the band calculation algorithm for the simplified CM in Figure 1.

The calculation of $\gamma_v(d)$ is dependent on other γ values. The two features of CMs previously mentioned (i.e. (1) no non-emitting loops and (2) $v <= y$ for y in C_v) enforce that, when calculating $\gamma_v(d)$ all γ_y values that $\gamma_v(d)$ is dependent on have been previously calculated. Intuitively, this constraint is satisfied because the algorithm calculates γ values as it moves up the model to progressively larger subtrees and longer subsequences, at each step requiring only γ values for shorter subsequences from states at or below the current one.

Bands are derived from the γ values as follows. The parameters $dmin_v$ and $dmax_v$ represent the minimum and maximum allowed subsequence lengths that can be aligned to the subtree at state v. These bounds are set such that:

$$\sum_{d=dmin_v}^{dmax_v} \gamma_v(d) \geq (1 - bandp)$$

This asserts that the probability that a subtree rooted at state v generates a subsequence of length at least $dmin_v$ and at most $dmax_v$ is above a specified probability threshold $(1 - bandp)$. Therefore, $bandp$ is the maximum allowable probability mass *outside* the band for any state in the model. Values of $bandp$ used are typically between 10^{-6} and 10^{-10}.

Importantly, $\gamma_v(d)$ values are only calculated for d up to a maximum sequence length of Z. Because CMs have emitting self-loops (i.e. insert states), there is no limit to the length of a sequence that can be generated from (i.e. aligned to) any subtree of the model that includes an insert state. However, calculation of the γ values neglect the probability that a subsequence of length $d > Z$ will be generated by any

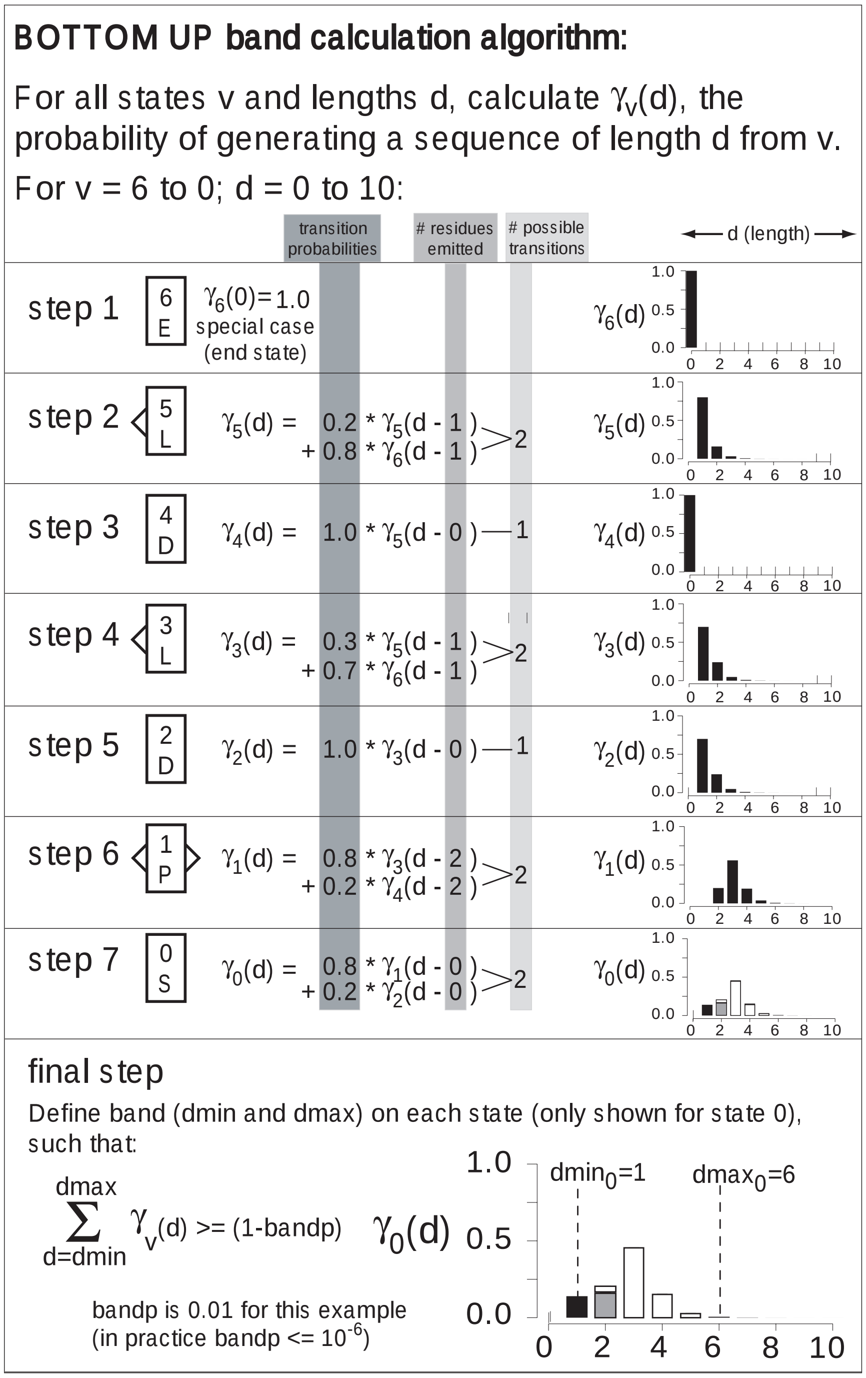

BOTTOM UP band calculation algorithm:
For all states v and lengths d, calculate $\gamma_v(d)$, the probability of generating a sequence of length d from v.
For v = 6 to 0; d = 0 to 10:
transition probabilities
# residues emitted
# possible transitions
d (length)
step 1 6 E $\gamma_6(0)=1.0$ special case (end state)
step 2 5 L $\gamma_5(d) = 0.2 * \gamma_5(d-1) + 0.8 * \gamma_6(d-1)$ 2
step 3 4 D $\gamma_4(d) = 1.0 * \gamma_5(d-0)$ 1
step 4 3 L $\gamma_3(d) = 0.3 * \gamma_5(d-1) + 0.7 * \gamma_6(d-1)$ 2
step 5 2 D $\gamma_2(d) = 1.0 * \gamma_3(d-0)$ 1
step 6 1 P $\gamma_1(d) = 0.8 * \gamma_3(d-2) + 0.2 * \gamma_4(d-2)$ 2
step 7 0 S $\gamma_0(d) = 0.8 * \gamma_1(d-0) + 0.2 * \gamma_2(d-0)$ 2
$\gamma_6(d)$ $\gamma_5(d)$ $\gamma_4(d)$ $\gamma_3(d)$ $\gamma_2(d)$ $\gamma_1(d)$ $\gamma_0(d)$
0.0 0.5 1.0
0 2 4 6 8 10
final step
Define band (dmin and dmax) on each state (only shown for state 0), such that:
$\sum_{d=dmin}^{dmax} \gamma_v(d) >= (1-bandp)$
bandp is 0.01 for this example (in practice bandp <= 10^{-6})
$dmin_0=1$
$dmax_0=6$

Figure 2: **A trace of the band calculation algorithm for the simplified CM in Figure 1.** The maximum length d considered (the Z parameter) is set as 10. Resulting γ probability distributions shown at right. For state 0 (step 7), the γ plot is color-coded to correspond with probabilities in Figure 1.

subtree. Therefore, Z must be sufficiently large such that the cumulative probability of all such subsequences is “negligible”. Our implementation handles this by enforcing that this cumulative probability is very small (?).

Using the band calculation to determine the maximum size of a hit to a CM

The W parameter is used during database search with CMs to define the maximum size of a hit to a model. Previous implementations required that the W parameter be manually set by the user. The band calculation algorithm delivers a probabilistically derived W for database search in $dmax_0$, which is the upper bound on the length of the entire sequence (the sequence generated by the top-most state, the root of the entire tree).

The banded CYK database search algorithm

Th CM CYK database search algorithm is different from the traditional CYK algorithm [25–27] in several important respects. First, while the traditional CYK is used with Chomsky normal form (CNF) grammars, the CM CYK is specially adapted for the CM grammar, which is not CNF. Secondly, CM CYK does not find the optimal parse tree of the entire input sequence, but rather scans the sequence and finds the set of non-overlapping subsequences (hits) that each align globally with respect to the model for which the summed score is maximized. Finally, transformed coordinates are used to allow a simple, memory efficient implementation of the scanning algorithm. Specifically, instead of the traditional i and j CYK coordinates for subsequence begin and end positions respectively, the CM CYK uses j and d coordinates with $d = j - i + 1$ [11].

The CM CYK search algorithm calculates $\alpha_v(j, d)$ - the log odds score of the most likely CM parse subtree rooted at state v that generates (aligns to) the length d subsequence $x_{j-d+1}..x_j$ of sequence x [11]. Similar to the band calculation algorithm, this calculation initializes at the smallest subtrees (E states) and shortest subsequences ($d = 0$) and iterates upward and outward to progressively larger subtrees and longer subsequences.

We accelerate CYK database search using bands ($dmin$ and $dmax$ values) derived from the band calculation algorithm. The bands correspond to state specific bounds on the d dimension of the α matrix that limit possible values of d (subsequence lengths) that can be aligned to each subtree of the model. The bands are applied by initializing all cells of the matrix outside the bands to a score of $-\infty$, and never reevaluating them during the recursion. The banded CYK database search algorithm is:

```
Initialization (impose bands): for $j = 0$ to $L$, $v = M$ down to 1:
    for $d = 0$ to $\min((dmin_v - 1), j)$    | $\alpha_v(j,d) = -\infty;$
    for $d = (dmax_v + 1)$ down to $j$        | $\alpha_v(j,d) = -\infty;$

Initialization at $d = 0$: for $j = 0$ to $L$, $v = M$ down to 1:
    $v =$ end state $(E)$:                    | $\alpha_v(j,0) = 0$
    $v =$ bifurcation $(B)$:                  | $\alpha_v(j,0) = \alpha_y(j,0) + \alpha_z(j,0)$
    $v =$ delete or start $(D,S)$:            | $\alpha_v(j,0) = \max_{y \in C_v}[\alpha_y(j,0) + \log t_v(y)];$
    else $(v = P,L,R)$                        | $\alpha_v(j,0) = -\infty$

Recursion: for $j = 1$ to $L, d = max(1, dmin_v)$ to $min(dmax_v, j), v = M$ down to 1
    $v =$ end state $(E)$:                    | $\alpha_v(j,d) = -\infty$
    $v =$ bifurcation $(B)$:                  | $kmin = max(dmin_z, (d - dmax_y))$
                                              | $kmax = min(dmax_z, (d - dmin_y))$
                                              | $\alpha_v(j,d) = \max_{kmin \leq k \leq kmax}[\alpha_y(j-k, d-k) + \alpha_z(j,k)];$
    $v =$ delete or start $(D,S)$:            | $\alpha_v(j,d) = \max_{y \in C_v}[\alpha_y(j,d) + \log t_v(y)];$
    else $(v = P,L,R)$ :                      | $\alpha_v(j,d) = \max_{y \in C_v}[\alpha_y(j - \Delta_v^R, d - (\Delta_v^L + \Delta_v^R)) + \log t_v(y)]$
                                              |         $+ \log e_v(x_i, x_j)$
```

For example, if we're calculating $\alpha_v(j,d)$ and v is a pair state (P), v will generate the basepair x_{j-d+1}, x_j and transit to a new state y (one of its possible transitions C_v) which then will have to account for the smaller subsequence $x_{j-d+2}..x_{j-1}$. The log odds score for a particular choice of next state y is the sum of three terms: an emission term $\log e_v(x_{j-d+1}, x_j)$, a transition term $\log t_v(y)$, and an already calculated solution for the smaller optimal parse tree rooted at y, $\alpha_y(j-1, d-2)$. The value assigned to $\alpha_v(j,d)$ is the maximum over all possible choices of child states y that v can transit to.

Tuning speed versus accuracy with the *bandp* parameter

The banded CM CYK algorithm offers acceleration by ignoring all alignments that violate the band of at least one state, and finds the optimal alignment consistent with all the bands. Therefore, when the globally optimal solution is not consistent with the bands, the acceleration comes at a cost to sensitivity. This is most likely to occur when aligning remote homologs, which may have significantly different subsequence lengths in some homologous regions. This speed versus accuracy tradeoff can be controlled to an extent by the *bandp* parameter. In general, higher *bandp* values will give tighter bands that result in faster, less sensitive searches than lower *bandp* values. Empirically, practical values of *bandp* are between 10^{-6} and 10^{-10} (see benchmark results).

Informative transition priors for appropriate band calculation

The band calculation algorithm uses only the transition probabilities of the model to determine the bands. These probabilities are themselves calculated as mean posterior estimates using observed counts from the input alignment and a Dirichlet prior [23]. Previous to this work, uninformative Dirichlet densities corresponding to Laplace "plus-1" pseudo-counts were used as transition priors. However, uninformative priors are problematic during band calculation because they do not accurately reflect the distributions that would be observed from actual RNA sequences, and result in inappropriate bands that would often ignore the optimal alignment. This problem is exacerbated when there are few training sequences, because the prior has more of an impact during mean posterior estimation. Figure depicts the effect of plus-1 priors on band calculation anecdotally for three RNA families by showing that the the bounds on the full length of potential new homologs ($dmin_0$ and $dmax_0$) do not appropriately reflect the lengths of the sequences in the input alignment.

To alleviate this problem, we estimated many (36) single component Dirichlet densities to be used as informative transition priors that accurately reflect characteristics of RNA sequences. The specific density used as a prior for mean posterior estimation of transition probabilities out of a given state v to potential states C_v is dependent on the node and state types of the states in C_v. The CM architecture allows exactly 73 possible "transition alphabets" of node and state types in C_v. Instead of estimating 73 Dirichlet densities, we defined 36 groups of transition alphabets by combining similar alphabets into the same group, and estimated a Dirichlet density for each group to be applied for all alphabets in the group. We derived training data for estimatiion of the Dirichlet densities from version 6.1 of the Rfam database [14]. Specifically, we built CMs from each of the 381 Rfam version 6.1 seed alignments and collected counts of the observed transitions used in the parse trees of each seed sequence. Table 1 contains statistics on the counts collected for each of the transition alphabets and groups of alphabets. Dirichlet densities were estimated from these counts using the maximum likelihood based method described in [13] with one exception, our procedure used a conjugate gradient descent algorithm [28] for optimization while [13] describes an expectation-maximization (EM) based approach. The resulting Dirichlet parameters are in Table 1. Incorporating the informative transition priors during mean posterior estimation of the transition probabilities has a dramatic impact on calculation of the bands as shown in Figure .

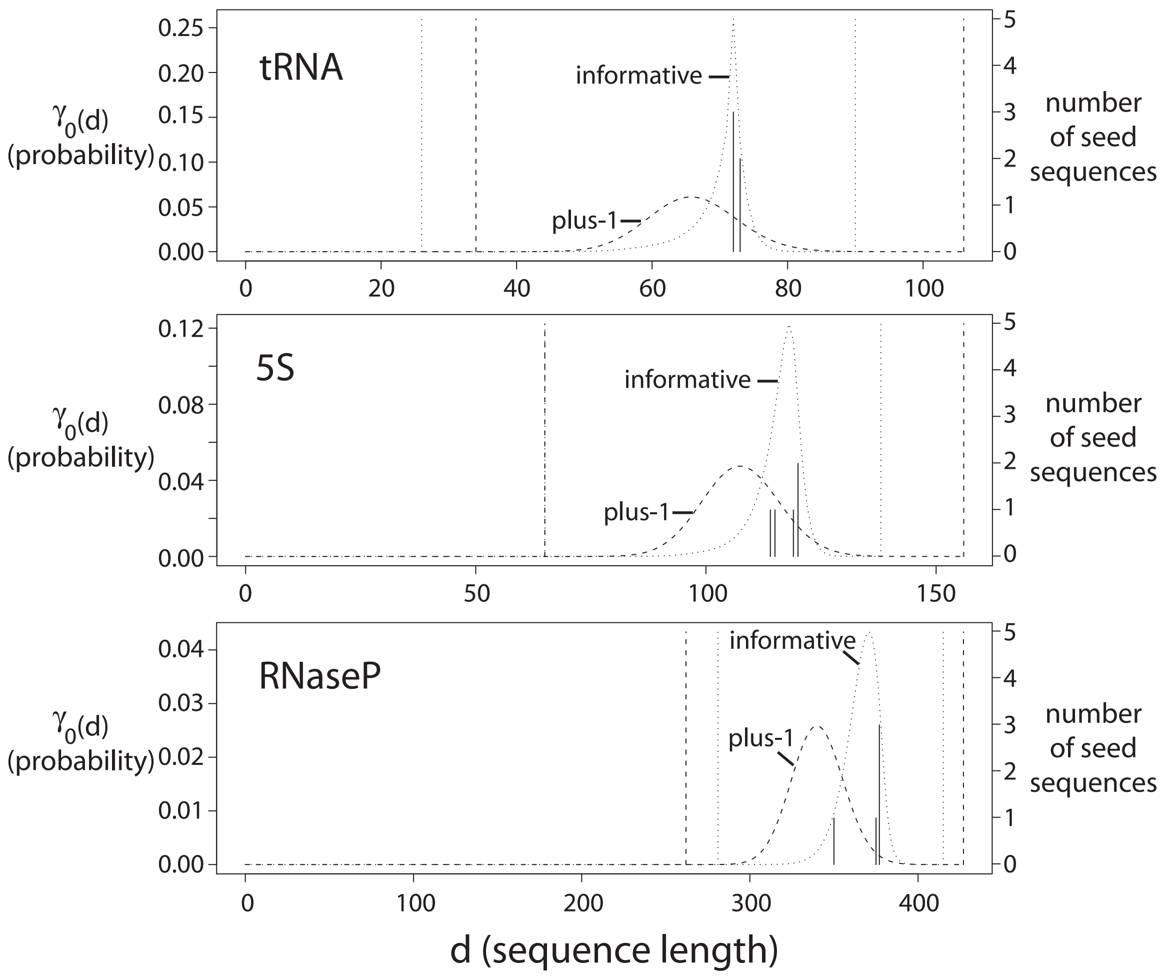

Figure 3: **Effect of transition priors on band calculation.** Solid vertical lines represent the lengths of the 5 training sequences in the alignment used to build each model, corresponding with the right vertical axis labels. Band calculation is compared using "plus-1" transition priors and the newly estimated "informative" Dirichlet priors as follows: Dashed probability distributions show $\gamma_0(d)$, the probability a sequence of length d is generated by (i.e. will be aligned to) state 0 (the top-most, root state) of each model. Dashed vertical lines indicate the band values ($dmin_0$ (left) and $dmax_0$ (right)) derived from the $\gamma_0(d)$ distribution using $bandp = 10^{-7}$ (the probability mass within each band is 99.99999%).

alph	grp	alph	grp	node	next	transition alphabets and Dirichlet α parameters												
#	#	counts	counts	state	node	$\|\alpha\|$	a	$\frac{\alpha_a}{\|\alpha\|}$	a	$\frac{\alpha_a}{\|\alpha\|}$	a	$\frac{\alpha_a}{\|\alpha\|}$	a	$\frac{\alpha_a}{\|\alpha\|}$	a	$\frac{\alpha_a}{\|\alpha\|}$	a	$\frac{\alpha_a}{\|\alpha\|}$
1		6	11	MATP_MP	BIF	0.5509	IL	0.1229	IR	0.0001	B	0.8770						
2		7023	7119	MATP_MP	MATP	7.2986	IL	0.0023	IR	0.0024	MP	0.9816	ML	0.0056	MR	0.0046	D	0.0035
3		1600	1830	MATP_MP	MATL	1.5914	IL	0.0179	IR	0.0155	ML	0.9200	D	0.0466				
4		145	195	MATP_MP	MATR	1.9038	IL	0.0173	IR	0.0073	MR	0.8903	D	0.0852				
5	1	2	11	MATP_MP	END	0.5509	IL	0.1229	IR	0.0001	E	0.8770						
6*		1	2	MATP_ML	BIF	3.0000	IL	0.3333	IR	0.3333	B	0.3333						
7		577	577	MATP_ML	MATP	0.6941	IL	0.0131	IR	0.0103	MP	0.4032	ML	0.4983	MR	0.0115	D	0.0636
8		133	133	MATP_ML	MATL	0.9316	IL	0.0739	IR	0.0651	ML	0.7038	D	0.1571				
9		15	15	MATP_ML	MATR	0.3272	IL	0.1884	IR	0.0432	MR	0.4082	D	0.3602				
10*	6	1	2	MATP_ML	END	3.0000	IL	0.3333	IR	0.3333	E	0.3333						
11*		1	2	MATP_MR	BIF	3.0000	IL	0.3333	IR	0.3333	B	0.3333						
12		531	531	MATP_MR	MATP	0.7987	IL	0.0079	IR	0.0190	MP	0.3241	ML	0.0193	MR	0.5631	D	0.0666
13		151	151	MATP_MR	MATL	0.6933	IL	0.0357	IR	0.0699	ML	0.3066	D	0.5879				
14		15	15	MATP_MR	MATR	0.3574	IL	0.0582	IR	0.0002	MR	0.7629	D	0.1787				
15*	11	1	2	MATP_MR	END	3.0000	IL	0.3333	IR	0.3333	E	0.3333						
16*		0	2	MATP_D	BIF	3.0000	IL	0.3333	IR	0.3333	B	0.3333						
17		575	575	MATP_D	MATP	0.5450	IL	0.0019	IR	0.0047	MP	0.0857	ML	0.0534	MR	0.0528	D	0.8015
18		149	149	MATP_D	MATL	0.5831	IL	0.0421	IR	0.0526	ML	0.2080	D	0.6973				
19		14	14	MATP_D	MATR	0.1164	IL	0.0001	IR	0.0001	MR	0.2439	D	0.7559				
20*	16	2	2	MATP_D	END	3.0000	IL	0.3333	IR	0.3333	E	0.3333						
21		2	4	MATP_IL	BIF	1.4397	IL	0.6553	IR	0.0445	B	0.3002						
22		121	126	MATP_IL	MATP	0.9402	IL	0.1673	IR	0.1394	MP	0.5904	ML	0.0443	MR	0.0259	D	0.0327
23		114	119	MATP_IL	MATL	0.8046	IL	0.3108	IR	0.1936	ML	0.4610	D	0.0346				
24		14	15	MATP_IL	MATR	1.0926	IL	0.1419	IR	0.0501	MR	0.6538	D	0.1541				
25	21	2	4	MATP_IL	END	1.4397	IL	0.6553	IR	0.0445	E	0.3002						
26		1	31	MATP_IR	BIF	0.9361	IR	0.2827	B	0.7173								
27		145	227	MATP_IR	MATP	1.5494	IR	0.1884	MP	0.7090	ML	0.0165	MR	0.0588	D	0.0273		
28		129	701	MATP_IR	MATL	1.6332	IR	0.3681	ML	0.5752	D	0.0566						
29		8	160	MATP_IR	MATR	1.2428	IR	0.2633	MR	0.6809	D	0.0558						
30	26	0	31	MATP_IR	END	0.9361	IR	0.2827	E	0.7173								
31		108	1130	MATL_ML	BIF	1.2298	IL	0.0078	B	0.9922								
32		420	1319	MATL_ML	MATP	2.4162	IL	0.0132	MP	0.9520	ML	0.0150	MR	0.0129	D	0.0070		
33		19013	19371	MATL_ML	MATL	1.8632	IL	0.0082	ML	0.9711	D	0.0207						
34		859	6692	MATL_ML	MATR	72.1283	IL	0.0058	MR	0.9755	D	0.0187						
35	31	801	1130	MATL_ML	END	1.2298	IL	0.0078	E	0.9922								
36		28	172	MATL_D	BIF	6.8008	IL	0.0029	B	0.9971								
37		103	103	MATL_D	MATP	0.7288	IL	0.0321	MP	0.5730	ML	0.0536	MR	0.1654	D	0.1758		
38		3152	3152	MATL_D	MATL	0.4101	IL	0.0138	ML	0.3105	D	0.6756						
39		154	154	MATL_D	MATR	0.6736	IL	0.0203	MR	0.6014	D	0.3782						
40	36	144	172	MATL_D	END	6.8008	IL	0.0029	E	0.9971								
41	26	13	31	MATL_IL	BIF	0.9361	IL	0.2827	B	0.7173								
42	27	35	227	MATL_IL	MATP	1.5494	IL	0.1884	MP	0.7090	ML	0.0588	MR	0.0165	D	0.0273		
43	28	549	701	MATL_IL	MATL	1.6332	IL	0.3681	ML	0.5752	D	0.0566						
44	29	45	160	MATL_IL	MATR	1.2428	IL	0.2633	MR	0.6809	D	0.0558						
45	26	0	31	MATL_IL	END	0.9361	IL	0.2827	E	0.7173								
46	31	206	1130	MATR_MR	BIF	1.2298	IR	0.0078	B	0.9922								
47	32	848	1319	MATR_MR	MATP	2.4162	IR	0.0132	MP	0.9520	ML	0.0150	MR	0.0129	D	0.0070		
48	34	5833	6692	MATR_MR	MATR	2.1283	IR	0.0058	MR	0.9755	D	0.0187						
49		39	39	MATR_D	BIF	0.4664	IR	0.0463	B	0.9537								
50		176	176	MATR_D	MATP	0.8689	IR	0.0245	MP	0.6126	ML	0.1269	MR	0.0471	D	0.1890		
51		771	771	MATR_D	MATR	0.4869	IR	0.0119	MR	0.3373	D	0.6507						
52	26	15	31	MATR_IR	BIF	0.9361	IR	0.2827	B	0.7173								
53	27	39	227	MATR_IR	MATP	1.5494	IR	0.1884	MP	0.7090	ML	0.0165	MR	0.0588	D	0.0273		
54	29	107	160	MATR_IR	MATR	1.2428	IR	0.2633	MR	0.6809	D	0.0558						
55		338	338	BEGL_S	MATP	5.0422	MP	0.9579	ML	0.0121	MR	0.0183	D	0.0117				
56	31	15	1130	BEGR_S	BIF	1.2298	IL	0.0078	B	0.9922								
57	32	51	1319	BEGR_S	MATP	2.4162	IL	0.0132	MP	0.9520	ML	0.0150	MR	0.0129	D	0.0070		
58	33	358	19371	BEGR_S	MATL	1.8632	IL	0.0082	ML	0.9711	D	0.0207						
59	26	2	31	BEGR_IL	BIF	0.9361	IL	0.2827	B	0.7173								
60	27	3	227	BEGR_IL	MATP	1.5494	IL	0.1884	MP	0.7090	ML	0.0588	MR	0.0165	D	0.0273		
61	28	19	701	BEGR_IL	MATL	1.6332	IL	0.3681	ML	0.5752	D	0.0566						
62	1	3	11	ROOT_S	BIF	0.5509	IL	0.1229	IR	0.0001	B	0.8770						
63	2	96	7119	ROOT_S	MATP	7.2986	IL	0.0023	IR	0.0024	MP	0.9816	ML	0.0056	MR	0.0046	D	0.0035
64	3	230	1830	ROOT_S	MATL	1.5914	IL	0.0179	IR	0.0155	ML	0.9200	D	0.0466				
65	4	50	195	ROOT_S	MATR	1.9038	IL	0.0173	IR	0.0073	MR	0.8903	D	0.0852				
66	21	0	4	ROOT_IL	BIF	1.4397	IL	0.6553	IR	0.0445	B	0.3002						
67	22	5	126	ROOT_IL	MATP	0.9402	IL	0.1673	IR	0.1394	MP	0.5904	ML	0.0443	MR	0.0259	D	0.0327
68	23	5	119	ROOT_IL	MATL	0.8046	IL	0.3108	IR	0.1936	ML	0.4610	D	0.0346				
69	24	1	15	ROOT_IL	MATR	1.0926	IL	0.1419	IR	0.0501	MR	0.6538	D	0.1541				
70	26	0	31	ROOT_IR	BIF	0.9361	IR	0.2827	B	0.7173								
71	27	5	227	ROOT_IR	MATP	1.5494	IR	0.1884	MP	0.7090	ML	0.0165	MR	0.0588	D	0.0273		
72	28	4	701	ROOT_IR	MATL	1.6332	IR	0.3681	ML	0.5752	D	0.0566						
73	29	0	160	ROOT_IR	MATR	1.2428	IR	0.2633	MR	0.6809	D	0.0558						

Table 1: **Transition alphabets and groups with corresponding training counts and estimated Dirichlet transition prior parameters.** "alph #"= transition alphabet number; "*" indicates a plus-1 prior is used. "grp #"= transition group number, each group is numbered as the lowest numbered alphabet in the group, this column is blank if alphabet number = group number. "alph counts"= observed Rfam 6.1 counts for alphabet. "grp counts"= total Rfam 6.1 counts for group, used to estimate a single component Dirichlet density for use as a prior for each alphabet in the group. "node state"= initial node state type for each alphabet. "next node"= type of immediately downstream node for each alphabet.

		# aln	# filtered	# consensus	# consensus	bp	SS
alignment	# seq	columns	seq	bp	SS columns	counts	counts
LSU	1551	7270	139	601	1532	65229	180558
SSU bap	12773	2653	254	421	680	97834	153565
SSU euk	7151	4558	207	407	959	72521	174260
SSU mito	1039	3791	107	216	524	19803	56510

Table 2: **Statistics on the alignments used for emission prior estimation.** LSU: large subunit ribosomal RNA; SSU: small subunit ribosomal RNA; "SSU bap" alignment contains bacterial, archaeal and plastid sequences.

Increasing sensitivity by refining CM parameterization

Informative emission priors

To complement the informative transition priors, Dirichlet density *mixtures* were estimated to use as informative emission priors. Although the emission probabilities do not affect band calculation, using Dirichlet density mixtures has been shown to improve the ability of profile HMMs to detect remote protein homology [13, 29], and we hoped to show a similar effect for CMs.

For emission prior estimation, observed counts of single-stranded and base-paired residues were collected from the individually structurally annotated ribosomal RNA alignments from the European Ribosomal RNA Database [30, 31]. Starting with four alignments from the 2002 version of the database, sequences were removed in which either less than 40% of the base paired positions are present or more than 5% of the nucleotides are ambiguous. Each resulting alignment was filtered so that no two sequences in a filtered alignment were greater than 80% identical. Characteristics of the filtered alignments and collected counts are in Table 2.

The counts were used to estimate two sets of Dirichlet mixtures, one for base pairs and one for single stranded residues, as described in [13]. We experimented with different numbers of components and finally decided on the 9 and 8 component mixtures for base pairs and singlets shown in Tables 3 and 4 respectively.

Model entropy weighting

We also extend the profile HMM "entropy weighting" technique to CMs to increase sensitivity. This technique is independent of the banded strategy, but takes advantage of the ability of informative emis-

component i	1	2	3	4	5	6	7	8	9
q_i	0.0305	0.0703	0.1185	0.1810	0.1888	0.1576	0.0417	0.0959	0.1156
$\lvert\alpha\rvert$	14.3744	2.9920	26.2757	0.5342	4.2716	13.3232	33.8619	22.2258	33.1991

ab	mean α	$\frac{\alpha_{ab}}{\lvert\alpha\rvert}$	$\frac{\alpha_{ab}}{\lvert\alpha\rvert}$	$\frac{\alpha_{ab}}{\lvert\alpha\rvert}$	$\frac{\alpha_{ab}}{\lvert\alpha\rvert}$	$\frac{\alpha_{ab}}{\lvert\alpha\rvert}$	$\frac{\alpha_{ab}}{\lvert\alpha\rvert}$	$\frac{\alpha_{ab}}{\lvert\alpha\rvert}$	$\frac{\alpha_{ab}}{\lvert\alpha\rvert}$	$\frac{\alpha_{ab}}{\lvert\alpha\rvert}$
AA	0.0063	0.0398	0.0390	0.0011	0.0017	0.0005	0.0062	0.0064	0.0058	0.0002
AC	0.0092	0.0421	0.0176	0.0009	0.0152	0.0018	0.0125	0.0115	0.0051	0.0046
AG	0.0052	0.0381	0.0226	0.0046	0.0034	0.0008	0.0032	0.0040	0.0053	0.0001
AU	**0.1663**	**0.1092**	0.0864	0.0194	**0.2138**	**0.1464**	**0.2563**	**0.7360**	**0.1295**	0.0404
CA	0.0086	0.0412	0.0510	0.0054	0.0027	0.0044	0.0018	0.0030	0.0138	0.0002
CC	0.0038	0.0327	0.0115	0.0030	0.0001	0.0003	0.0036	0.0039	0.0035	0.0041
CG	**0.2412**	**0.1007**	**0.1392**	**0.8310**	**0.1359**	**0.3211**	0.0889	0.0340	**0.2870**	0.0147
CU	0.0066	0.0418	0.0172	0.0027	0.0104	0.0019	0.0045	0.0076	0.0052	0.0003
GA	0.0061	0.0362	0.0266	0.0002	0.0074	0.0002	0.0058	0.0045	0.0042	0.0021
GC	**0.2547**	**0.1299**	0.0544	0.0206	**0.1786**	**0.1613**	**0.4079**	0.0945	**0.1155**	**0.8858**
GG	0.0063	0.0327	0.0142	0.0045	0.0091	0.0005	0.0072	0.0023	0.0044	0.0030
GU	0.0567	0.0811	0.0412	0.0049	**0.1355**	0.0451	0.0668	0.0303	0.0356	0.0218
UA	**0.1571**	**0.1063**	**0.3085**	0.0672	**0.1856**	**0.2293**	0.0902	0.0363	**0.3108**	0.0151
UC	0.0063	0.0477	0.0263	0.0006	0.0048	0.0002	0.0056	0.0042	0.0060	0.0038
UG	0.0543	0.0746	**0.1054**	0.0317	0.0807	0.0814	0.0299	0.0120	0.0551	0.0032
UU	0.0114	0.0459	0.0389	0.0022	0.0151	0.0048	0.0098	0.0095	0.0133	0.0008

Table 3: **Parameters of the 9 component Dirichlet mixture emission prior for base pairs.** q_i = mixture coefficient for component i. Normalized α values > 0.10 are in bold faced type.

component i	1	2	3	4	5	6	7	8
q	0.0851	0.0159	0.1020	0.4160	0.0745	0.0554	0.1184	0.1327
$\|\alpha\|$	15.4467	154.4640	180.2862	5.4562	0.2199	16.4089	13.4592	19.9059

a	mean α	$\frac{\alpha_a}{\|\alpha\|}$	$\frac{\alpha_a}{\|\alpha\|}$	$\frac{\alpha_a}{\|\alpha\|}$	$\frac{\alpha_a}{\|\alpha\|}$	$\frac{\alpha_a}{\|\alpha\|}$	$\frac{\alpha_a}{\|\alpha\|}$	$\frac{\alpha_a}{\|\alpha\|}$	$\frac{\alpha_a}{\|\alpha\|}$
A	**0.3951**	0.0373	**0.9961**	**0.9787**	**0.3109**	**0.3383**	0.0375	0.0864	**0.8247**
C	**0.1635**	0.0490	0.0015	0.0052	**0.2067**	**0.1782**	**0.8916**	0.0303	0.0493
G	**0.2041**	0.0220	0.0023	0.0072	**0.1751**	**0.2905**	0.0182	**0.8313**	0.0569
U	**0.2372**	**0.8917**	0.0000	0.0090	**0.3073**	**0.1930**	0.0527	0.0519	0.0691

Table 4: **Parameters of the 8 component Dirichlet mixture emission prior for singlets.** q_i = mixture coefficient for component i. Normalized α values > 0.10 are in bold faced type.

sion priors to accurately reflect characteristics of real RNA sequences. The key idea of entropy weighting is to scale the contribution of the observed counts from the input alignment relative to the prior during mean posterior estimation. The specific scaling factor is determined such that a target model entropy is reached. We heuristically define a model's entropy as the mean match state entropy, with match state entropy defined as $\sum_a e_v(a) \log \frac{1}{e_v(a)}$ (P states are treated as two match states). Notably, this definition ignores any contribution from insert emissions or transitions of the model. The default target model entropy used in INFERNAL is 1.46 bits (because using this value gave the best results for our benchmark), but this value can be set by the user.

An Rfam based benchmark

To assess the performance impact of the bands, informative priors, and entropy weighting on homology search, we designed a benchmark based on the Rfam database [14]. Rfam version 7.0 families were selected for the benchmark that exhibit a broad range of primary sequence divergence. For each of these families, a cluster of highly similar sequences was used as a training input alignment (preserving the Rfam alignment) and another cluster of sequences sufficiently dissimilar from the training set was defined as the test set. These designations were made following single-linkage clustering of each family based on percent identity given the alignment. To qualify for the benchmark, a family was required to contain possible training and testing sets with the following properties:

- no training and test sequences are greater than 60% identical given the Rfam alignment.
- no two test sequences are greater than 70% identical given the Rfam alignment.
- training sets have at least 5 sequences.

51 families satisfy these criteria (listed in Table 6). The total number of test sequences across the 51 families is 450, with a combined length of 101,855 nt.

The CM CYK database search algorithm is designed for homology search in genomic sequence, motivating the fabrication of a "pseudo-genome" for our benchmark. To limit the time necessary for carrying out the benchmark, the length of the pseudo-genome is only 1 million bases (MB); organized into twenty 50 kilobase (KB) chromosomes. The pseudo-genome was constructed by first generating the 20 chromosomes using a 0th order single state Markov model with equiprobable emission probabilities of 0.25 for the four letter DNA emission alphabet of $\{A, C, G, T\}$. The 450 test sequences were embedded into the genome by randomly chosing a chromosome, orientation, and starting position. No two test sequences were permitted to overlap on either strand.

The benchmark is performed for INFERNAL by first building a CM for each family using its training seed alignment. The pseudo-genome is then searched with each CM in *local* mode. BLAST was also tested; for each family, each training sequence is used as a query sequence to search the pseudo-genome. For each benchmark run, the hits returned for each of the 51 families were sorted based on score into a ranked family specific list. Using these 51 lists, a master list was created, with all hits across families sorted by score.

For BLAST, hits with an E-value less than 1.0 were sorted from low to high. For INFERNAL, all hits greater than 8 bits were sorted from high to low bit score. Each hit in a ranked list was classified into one of three categories:

positives: hits returned when searching for family X test sequences that *significantly overlap* with one of the true family X test sequences. For BLAST, only the lowest E-value positive hit to each true test sequence is counted.

ignores: hits using family X as a query that *significantly overlap* with a true test sequence from family Y (where Y != X) on either strand of the chromosome.

negatives: hits that are not postives or ignores. For any two negatives that *significantly overlap*, the one with the better score is counted.

We define *significant overlap* as the case when the length of overlap between two sequences (either two hits, or one hit and one test sequence embedded in the pseudo-genome) is more than 50% the length of the shorter of the two sequences.

Benchmark MER statistics

The minimum error rate (MER) statistic [32] (is this citation correct?) was used to measure benchmark performance. The MER threshold is defined as a score, a point in the ranked list of hits, at which the sum of the false positives (FPs, hits classified as *negatives* with scores better than the threshold) and false negatives (FNs, the number of true test sequences for which there are no corresponding *positives* with scores better than the threshold) is minimized. The MER of a method is defined as the sum of false positives and false negatives at the MER threshold. Lower MERs are better.

Observed acceleration from bands

Figure 4 shows the levels of acceleration for each of the 51 families in the benchmark set for two different values of the $bandp$ parameter. The banded strategy offers between a 1.1 (for the IRE family) and 14.5 (for the CsrB family) fold speed-up relative to a non-banded search. The level of acceleration roughly scales with the average sequence length of the family being modelled, although other factors, including variation in substructure lengths and number of bifurcations also impact acceleration. The length dependent effect occurs because the number of non-banded alignments considered per state of the model is $O(L^2)$, while the number of banded alignments per state considered is $O(kL)$ with k equal to the average band width across all M states ($(\sum_v dmax_v - dmin_v + 1)/M$), which varies slightly across families but independently of their lengths. The average family speed-up factor for benchmark set is 3.17 and 4.75 for $bandp$ values of 10^{-10} and 10^{-6} respectively. The total speed-up factor for searching for all families is 4.40 and 6.74 for $bandp$ values of 10^{-10} and 10^{-6} respectively.

These timings do not consider the time required for band calculation. The bands can be calculated *a priori*, independent of the database, in a matter of seconds (about 10 seconds for SSU rRNA, the largest RNA family tested) which is negligible considering the running time of a search is typically on the order of hours or days.

Benchmark performance

Acceleration from the banded approach is not useful it comes at a significant cost to sensitivity. To measure the extent of this cost, *summary* MER statistics were calculated from the master lists of hits to describe the performance of a method if a single threshold must be chosen for all families (and that threshold could be chosen *after* the results are collected). This score threshold may be used in future searches, hopefully resulting in similar sensitivity and specificity measures. Additionally, *family specific* MER statistics were calculated from the family specific lists of hits, which explain the performance that could be achieved if different optimal thresholds were used for each family. Table 5 lists the summary MER statistic, and family-specific MER statistics (the sum over all 51 families) for each method tested. Table 6 contains the individual family-specific MER statistics of selected methods. Figure 5 displays the benchmark performance of the various methods differently, as a ROC plot with sensitivity and specificity measures for every possible cut point threshold in the master ranked list of hits (each method from Table 5 except for row 3 is included in the Figure 5 ROC plot).

	program	prior	entropy (bits)	$bandp$	summary MER	family-specific MER
1	BLAST	-	-	-	216	188
2	INFERNAL	plus-1	-	-	230	184
3	INFERNAL	informative	-	-	188	163
4	INFERNAL	informative	1.46	-	104	90
5	INFERNAL	informative	1.46	10^{-6}	116	98
6	INFERNAL	informative	1.46	10^{-10}	110	94

Table 5: **Rfam benchmark MER summary statistics.** prior: “plus-1” if uninformative Laplace plus-1 priors were used; “informative” if new Dirichlet priors were used. entropy: target model entropy in bits for entropy weighting; “-” if entropy weighting was not used. “$bandp$”: tail probability loss for banded calculation used; “-” if search was non-banded. summary MER: MER across 51 benchmark families; family-specific MER: MER for each family, summed over all 51 families. Program versions: Row 1: WU-BLASTN-2.0MP –kap -W=7. Row 2: INFERNAL version 0.55. Rows 3-6: INFERNAL version 0.70.

Discussion

The benchmark results summarized in Tables 5 and 6 and Figures 4 and 5 demonstrate the following:

- **The informative priors alone boost performance.** Incorporating the new priors drops the summary MER from 230 to 188, and the family specific MER from 184 to 163 (Table 5, row 2 versus 3). Figure 5 demonstrates that the sensitivity increase does not sacrifice specificity.
- **Entropy weighting significantly elevates performance.** Enforcing a target model entropy brings the summary MER from 188 down to 104, and the family specific MER from 163 down to 90. (Table 5, row 4 versus row 2). Figure 5 demonstrates that the sensitivity increase does not sacrifice specificity. (THIS IS MISLEADING, THE EL SELF TRANSITION ALSO CHANGES BETWEEN THESE ROWS).
- **The banded strategy offers acceleration with a small cost to performance.** Using a $bandp$ of 10^{-6} results in an average speed-up per family of 4.75 fold and a total speed-up of 6.74 fold for the entire benchmark set (Table 6). This speed up increases summary MER from 104 to 116 and

the family specific MER from 90 to 98 (Table 5, rows 6 versus row 5). A $bandp$ of 10^{-10} gives a smaller 3.17 fold average and 4.40 fold total acceleration (Table 6 at a smaller cost to performance; the summary MER is 110 and the family MER is 94 (row 7 versus row 5). Figure 5 is perhaps more informative, showing sensitivity as a function of specificity.

We have presented separate techniques to improve the speed and sensitivity of CM based homology search. The informative prior distributions are central to both of these improvements. Informative transitions priors are critical to the band calculation (Figure), and informative emission priors allow effective model entropy weighting. Our training datasets for prior estimation are not ideal: very few counts were used to estimate many of the transition priors (Table 1), and only ribosomal RNA alignments were used for to derive counts for the emission priors. We were driven to both datasets by a lack of better options. Despite this, the resulting priors seem to perform well. We hope that the CM methods we have improved on here will help to provide better training data for future tools. While we recognize that this approach of building tools using sparse data to amass better data for use in tool building is circular, we feel that such an approach is necessary in this case (?).

The model entropy weighting strategy has important implications for profile HMM filtering methods that rely on primary sequence conservation. When building a CM from an input training alignment with many highly identical sequences, entropy weighting will create a model with lower information content than a model built using previous methods (i.e. without entropy weighting). This is because the weight of the observations from the input alignment will be scaled down relative to the prior during parameterization. Profile HMM filters built from such CMs will also tend to have low information content. In general, these models will give higher scores (relative to models with higher information content) to sequences with lowers sequence identity to the training sequences, making them less efficient filters. In contrast, entropy weighting will not affect an initial filtering step by BLAST, as this step is completely independent of the CM. However, the overall sensitivity of a BLAST filtering approach may be increased, but only if the more sensitive entropy weighted CM finds hits in the filtered fraction that would be missed by CMs built without entropy weighting.

We believe the most important contribution of this work is the *a priori* banded strategy for accelerating CM homology search. A filtering approach and the banded strategy are complementary; the former reduces the search space for the expensive CM search, and the latter makes CM search less expensive. The band calculation method presented here is only one potential method for determining bands. There are certainly many others. The banded CM CYK database algorithm can use bands on subsequence lengths derived from any method. However, the band calculation method we present is ideal for homology search in one important respect. Because the bands are sequence independent and are determined solely from the transition probabilities of the model, they can be calculated once, in a few seconds prior to searching, adding a relatively negligible amount of time to the overall search. Other potential banded strategies that consider the sequence (like Brown's profile HMM based method in RNACAD [22]) need to continuously recalculate the bands as the database is scanned. Even so, we feel that sequence dependent banding strategies are promising for accelerating CM methods, and are currently exploring such techniques. As complementary filtering and banding methods continue to mature, we hope CM homology search will become more practical and widespread, contributing meaningfully to the understanding of non-coding RNAs.

Acknowledgements

EPN gratefully acknowledges financial support from NIH training grant X.

Rfam 7.0	family	#	#	mean len	BLAST					INFERNAL				
ID	name	train	test	(train)	MER	TP	FP	FN	thr	MER	TP	FP	FN	thr
RF00002	5_8S_rRNA	62	1	151	0	1	0	0	0.0045	0	1	0	0	11.27
RF00003	U1	46	6	159	2	4	0	2	0.049	0	6	0	0	12.26
RF00004	U2	76	1	184	0	1	0	0	0.017	0	1	0	0	10.00
RF00005	tRNA	1080	19	73	18	1	0	18	0.021	6	13	0	6	14.09
RF00008	Hammerhead_3	82	1	55	1	0	0	1	0.3	0	1	0	0	14.70
RF00009	RNaseP_nuc	26	21	320	19	2	0	19	0.02	17	4	0	17	11.67
RF00010	RNaseP_bact_a	233	1	332	0	1	0	0	0.00086	0	1	0	0	12.61
RF00011	RNaseP_bact_b	30	1	366	0	1	0	0	0.63	0	1	0	0	12.32
RF00012	U3	6	5	212	3	2	0	3	0.044	2	3	0	2	16.86
RF00015	U4	25	1	141	1	0	0	1	0.04	1	0	0	1	13.44
RF00017	SRP_euk_arch	28	21	303	19	2	0	19	0.52	7	14	0	7	12.84
RF00018	CsrB	8	1	351	0	1	0	0	0.0	0	1	0	0	12.97
RF00019	Y	15	1	94	1	0	0	1	0.073	1	0	0	1	15.10
RF00020	U5	29	3	115	1	2	0	1	0.054	0	3	0	0	13.64
RF00023	tmRNA	19	40	334	6	34	0	6	0.081	9	31	0	9	13.14
RF00024	Telomerase-vert	20	11	436	0	11	0	0	0.92	0	11	0	0	11.30
RF00025	Telomerase-cil	10	2	157	2	0	0	2	0.005	2	0	0	2	13.97
RF00028	Intron_gpI	5	24	300	20	4	0	20	0.92	13	11	0	13	12.25
RF00029	Intron_gpII	7	11	141	6	5	0	6	0.098	1	10	0	1	11.08
RF00030	RNase_MRP	18	3	284	3	0	0	3	0.003	3	0	0	3	12.46
RF00031	SECIS	11	24	64	23	1	0	23	0.71	13	13	2	11	14.58
RF00033	MicF	8	1	93	0	1	0	0	0.49	0	1	0	0	13.17
RF00037	IRE	36	1	28	1	0	0	1	0.995	1	0	0	1	14.98
RF00040	me5	6	1	338	0	1	0	0	0.89	0	1	0	0	11.78
RF00054	U25	5	1	87	1	0	0	1	0.68	1	0	0	1	16.66
RF00055	snoZ37	5	1	94	1	0	0	1	0.75	1	0	0	1	13.96
RF00059	THI	228	8	109	2	6	0	2	0.0018	0	8	0	0	13.66
RF00066	U7	28	2	62	0	2	0	0	0.49	0	2	0	0	14.23
RF00067	U15	9	3	146	1	2	0	1	0.13	1	2	0	1	22.46
RF00080	yypP-ykoY	20	33	129	29	5	1	28	0.11	1	32	0	1	17.84
RF00096	U8	5	1	135	0	1	0	0	0.024	0	1	0	0	13.25
RF00101	SraC_RyeA	6	1	250	0	1	0	0	0.2	0	1	0	0	11.87
RF00104	mir-10	9	2	73	2	0	0	2	0.17	2	0	0	2	16.13
RF00114	S15	10	1	117	1	0	0	1	0.029	1	0	0	1	16.94
RF00163	Hammerhead_1	65	1	68	1	0	0	1	0.36	0	1	0	0	16.52
RF00165	Corona_pk3	10	1	63	1	0	0	1	0.82	1	0	0	1	14.72
RF00167	Purine	33	4	99	0	4	0	0	0.13	0	4	0	0	13.02
RF00168	Lysine	33	17	180	4	13	0	4	0.036	0	17	0	0	15.98
RF00169	SRP_bact	46	15	96	3	12	0	3	0.08	0	15	0	0	14.22
RF00170	msr	5	3	70	3	0	0	3	0.49	3	0	0	3	13.49
RF00174	Cobalamin	87	66	203	0	66	0	0	0.021	0	66	0	0	15.90
RF00177	SSU_rRNA_5	145	21	593	3	19	1	2	0.58	0	21	0	0	9.89
RF00206	U54	12	1	81	1	0	0	1	0.054	1	0	0	1	15.80
RF00213	snoR38	7	3	88	1	2	0	1	0.49	0	3	0	0	16.07
RF00230	T-box	10	35	244	4	31	0	4	0.9992	1	34	0	1	12.34
RF00234	glmS	8	3	181	0	3	0	0	0.16	0	3	0	0	11.88
RF00373	RNaseP_arch	20	13	290	1	12	0	1	0.003	0	13	0	0	19.39
RF00379	ydaO-yuaA	31	4	147	0	4	0	0	0.026	0	4	0	0	13.11
RF00380	ykoK	35	3	168	0	3	0	0	0.073	0	3	0	0	13.13
RF00448	IRES_EBNA	7	1	213	0	1	0	0	0.79	1	0	0	1	11.99
RF00504	gcvT	109	5	102	3	2	0	3	0.04	0	5	0	0	13.40
MER statistics summed across all families					188	264	2	186	N/A	90	362	2	88	N/A
Summary MER statistics (using one threshold for all families)					216	240	6	210	0.017	104	354	8	96	16.38

Table 6: **Rfam benchmark families with MER statistics.** The minimum error rate (MER) threshold is the score for a given method searching for a given Rfam family at which the sum of false positives (FP) and false negatives (FN) is minimized. "MER"= FP+FN at threshold. "TP"= TP at threshold. "thr"= threshold; E-value (BLAST) or bit score (INFERNAL). For the row labelled "Summary MER statistics": MER statistics are derived from ranked list of all hits across all families. "mean len (train)" = mean length of training sequences in benchmark set. Program versions and options used: BLAST= WU-BLASTN-2.0MP –kap -W=7. INFERNAL= cmsearch –local (version 0.70)

					$bandp = 10^{-10}$		$bandp = 10^{-6}$		non-banded
Rfam ID	family	avg len	W	bifs	time	spd up	time	spd up	time
RF00177	SSU_rRNA_5	593	791	12	17.36	8.76	11.07	13.74	152.08
RF00024	Telomerase-vert	436	757	2	10.33	6.21	6.75	9.50	64.09
RF00011	RNaseP_bact_b	366	638	9	8.76	7.16	5.75	10.91	62.69
RF00018	CsrB	351	439	10	5.32	9.47	3.47	14.51	50.37
RF00040	rne5	338	369	4	5.88	6.27	4.13	8.93	36.88
RF00023	tmRNA	334	648	4	5.70	7.63	3.99	10.89	43.46
RF00010	RNaseP_bact_a	332	881	7	7.94	7.49	5.06	11.77	59.52
RF00009	RNaseP_nuc	320	709	4	18.13	2.89	10.78	4.86	52.40
RF00017	SRP_euk_arch	303	339	3	6.26	4.37	4.36	6.27	27.34
RF00028	Intron_gpI	300	460	4	8.98	3.51	5.40	5.85	31.55
RF00373	RNaseP_arch	290	439	4	7.39	3.73	4.96	5.57	27.58
RF00030	RNase_MRP	284	460	5	7.65	4.62	4.86	7.27	35.36
RF00101	SraC_RyeA	250	276	4	3.73	4.62	2.54	6.76	17.20
RF00230	T-box	244	338	1	4.37	3.51	2.86	5.36	15.32
RF00448	IRES_EBNA	213	246	4	2.90	4.34	1.98	6.36	12.57
RF00012	U3	212	236	2	3.56	3.70	2.53	5.20	13.16
RF00174	Cobalamin	203	458	3	7.33	2.29	4.34	3.87	16.81
RF00004	U2	184	219	4	2.45	4.37	1.75	6.11	10.72
RF00234	glmS	181	434	3	4.48	3.21	2.85	5.04	14.36
RF00168	Lysine	180	277	3	3.32	3.16	2.22	4.74	10.51
RF00380	ykoK	168	208	2	2.83	2.77	1.94	4.05	7.85
RF00003	U1	159	184	3	1.93	4.04	1.38	5.64	7.78
RF00025	Telomerase-cil	157	202	2	2.21	3.37	1.58	4.72	7.44
RF00002	5_8S_rRNA	151	224	2	2.22	2.95	1.53	4.28	6.54
RF00379	ydaO-yuaA	147	317	3	4.09	1.97	2.48	3.26	8.07
RF00067	U15	146	187	0	2.31	2.13	1.54	3.20	4.92
RF00015	U4	141	289	3	2.39	2.81	1.56	4.32	6.72
RF00029	Intron_gpII	141	286	1	3.23	2.67	2.05	4.21	8.62
RF00096	U8	135	198	2	2.14	2.52	1.43	3.77	5.38
RF00080	yybP-ykoY	129	287	2	2.62	2.11	1.75	3.16	5.53
RF00114	S15	117	138	1	1.41	2.31	1.00	3.26	3.26
RF00020	U5	115	141	1	1.57	2.32	1.18	3.08	3.63
RF00059	THI	109	305	2	3.68	1.67	2.23	2.75	6.14
RF00504	gcvT	102	298	1	3.48	1.23	2.14	2.01	4.30
RF00167	Purine	99	114	1	1.30	1.99	0.92	2.82	2.60
RF00169	SRP_bact	96	117	0	1.49	1.72	1.04	2.46	2.57
RF00019	Y	94	142	0	1.66	1.50	1.16	2.16	2.49
RF00055	snoZ37	94	117	0	1.21	1.65	0.86	2.33	1.99
RF00033	MicF	93	126	1	1.13	1.98	0.82	2.71	2.23
RF00213	snoR38	88	169	0	1.68	1.46	1.09	2.24	2.45
RF00054	U25	87	107	0	1.05	1.58	0.74	2.25	1.66
RF00206	U54	81	135	0	1.24	1.31	0.83	1.96	1.62
RF00005	tRNA	73	186	2	1.12	2.04	0.72	3.17	2.29
RF00104	mir-10	73	100	0	1.16	1.31	0.86	1.75	1.51
RF00170	msr	70	135	0	1.03	1.48	0.71	2.15	1.52
RF00163	Hammerhead_1	68	238	1	2.33	1.21	1.34	2.10	2.82
RF00031	SECIS	64	97	0	0.90	1.37	0.70	1.76	1.24
RF00165	Corona_pk3	63	78	0	0.68	1.43	0.52	1.85	0.97
RF00066	U7	62	96	0	0.74	1.39	0.55	1.87	1.03
RF00008	Hammerhead_3	55	164	1	1.07	1.16	0.67	1.85	1.24
RF00037	IRE	28	41	0	0.28	1.09	0.21	1.42	0.30
average					3.88	3.17	2.53	4.75	17.07
total					198.02	4.40	129.18	6.74	870.68

Table 7: **Statistics and running times for INFERNAL version 0.70 CMs on the Rfam benchmark.** "bifs"= number of bifurcations in consensus secondary structure. "time": hours per MB. "spd up": speed-up factor relative to non-banded. All searches performed in local mode.

References

[1] TM Lowe, SR Eddy: **tRNAscan-SE: A program for improved detection of transfer RNA genes in genomic sequence**. *Nucl. Acids Res.* 1997, **25**: 955–964.

[2] TM Lowe, SR Eddy: **A computational screen for methylation guide snoRNAs in yeast**. *Science* 1999, **283**: 1168–1171.

[3] EC Lai, P Tomancak, RW Williams, GM Rubin: **Computational identification of drosophila microRNA genes**. *Genome Biol.* 2003, **4**: R42.

[4] LP Lim, ME Glasner, S Yekta, CB Burge, DP Bartel: **Vertebrate microRNA genes**. *Science.* 2003, **299**: 1540.

[5] M Regalia, MA Rosenblad, T Samuelsson: **Prediction of signal recognition particle RNA genes**. *Nucleic Acids Res.* 2002, **30**: 3368–3377.

[6] MD Ermolaeva, HG Khalak, O White, HO Smith, SL Salzberg: **Prediction of transcription terminators in bacterial genomes**. *J Mol Biol.* 2000, **301**: 27–33.

[7] TJ Macke, DJ Ecker, RR Gutell, D Gautheret, DA Case, R Sampath: **RNAMotif, an RNA secondary structure definition and search algorithm**. *NAR* 2001, **29**: 4724–4735.

[8] D Gautheret, A Lambert: **Direct RNA motif definition and identification from multiple sequence alignments using secondary structure profiles**. *J. Mol. Biol.* 2001, **313**: 1003–1011.

[9] SR Eddy, R Durbin: **RNA sequence analysis using covariance models**. *Nucl. Acids Res.* 1994, **22**: 2079–2088.

[10] Y Sakakibara, M Brown, R Hughey, IS Mian, K Sjolander, RC Underwood, D Haussler: **Stochastic context-free grammars for tRNA modeling**. *Nucl. Acids Res.* 1994, **22**: 5112–5120.

[11] R Durbin, SR Eddy, A Krogh, GJ Mitchison: **Biological Sequence Analysis: Probabilistic Models of Proteins and Nucleic Acids**. Cambridge UK, Cambridge University Press 1998.

[12] SR Eddy: **A memory-efficient dynamic programming algorithm for optimal alignment of a sequence to an RNA secondary structure**. *BMC Bioinformatics* 2002, **3**: 18.

[13] K Sjolander, K Karplus, M Brown, R Hughey, A Krogh, IS Mian, D Haussler: **Dirichlet mixtures: A method for improving detection of weak but significant protein sequence homology**. *Comput. Applic. Biosci.* 1996, **12**: 327–345.

[14] S Griffiths Jones, S Moxon, M Marshall, A Khanna, SR Eddy, A Bateman: **Rfam: Annotating non-coding RNAs in complete genomes**. *Nucl. Acids Res.* 2005, **33**: D121–D141.

[15] Z Weinberg, WL Ruzzo: **Exploiting conserved structure for faster annotation of non-coding RNAs without loss of accuracy**. *Bioinformatics.* 2004, **20**: 334–341.

[16] Z Weinberg, WL Ruzzo: **Faster genome annotation of non-coding rna families without loss of accuracy**. *RECOMB '04* 2004, : 243–251.

[17] Z Weinberg, WL Ruzzo: **Sequence-based heuristics for faster annotation of non-coding RNA families**. *Bioinformatics.* 2006, **1**: 35–39.

[18] SF Altschul, W Gish, W Miller, EW Myers, DJ Lipman: **Basic local alignment search tool**. *J. Mol. Biol.* 1990, **215**: 403–410.

[19] DH Mathews: **Predicting a set of minimal free energy RNA secondary structures common to two sequences**. *Bioinformatics* 2005, **21**: 2246–2253.

[20] I Holmes: **Accelerated probabilistic inference of RNA structure evolution**. *BMC Bioinformatics* 2005, **6**: 73.

[21] D Sankoff: **Simultaneous solution of the RNA folding, alignment, and protosequence problems**. *SIAM J. Appl. Math.* 1985, **45**: 810–825.

[22] MP Brown: **Small subunit ribosomal RNA modeling using stochastic context-free grammars**. *Proc. Int. Conf. on Intelligent Systems in Molecular Biology* 2000, **8**: 57–66.

[23] SR Eddy: **The infernal user's guide**. [http://infernal.wustl.edu/] 2003.

[24] RJ Klein, SR Eddy: **RSEARCH: finding homologs of single structured RNA sequences**. *BMC Bioinformatics* 2003, **4**: 44.

[25] T Kasami: **An efficient recognition and syntax algorithm for context-free algorithms**. Technical Report AFCRL-65-758 Air Force Cambridge Research Lab Bedford, Mass. 1965.

[26] DH Younger: **Recognition and parsing of context-free languages in time n^3**. *Information and Control* 1967, **10**: 189–208.

[27] JE Hopcroft, JD Ullman: **Introduction to Automata Theory, Languages, and Computation**. Addison-Wesley 1979.

[28] WH Press, SA Teukolsky, WT Vetterling, BP Flannery: **Numerical Recipes in C: The Art of Scientific Computing**. Cambridge University Press 1993.

[29] M Brown, R Hughey, A Krogh, IS Mian, K Sjolander, D Haussler: **Using dirichlet mixture priors to derive hidden markov models for protein families**. *Proc Int Conf Intell Syst Mol Biol.* 1993, **1**: 47–55.

[30] YV de Peer, PD Rijk, J Wuyts, T Winkelmans, RD Wachter: **The european small subunit ribosomal RNA database**. *Nucleic Acids Res.* 2000, **28**: 175–176.

[31] J Wuyts, PD Rijk, YV de Peer, T Winkelmans, RD Wachter: **The European large subunit ribosomal RNA database**. *Nucl. Acids Res.* 2001, **29**: 175–177.

[32] WR Pearson: **Comparison of methods for searching protein sequence databases**. *Protein Sci.* 1995, **4**: 1145–1160.

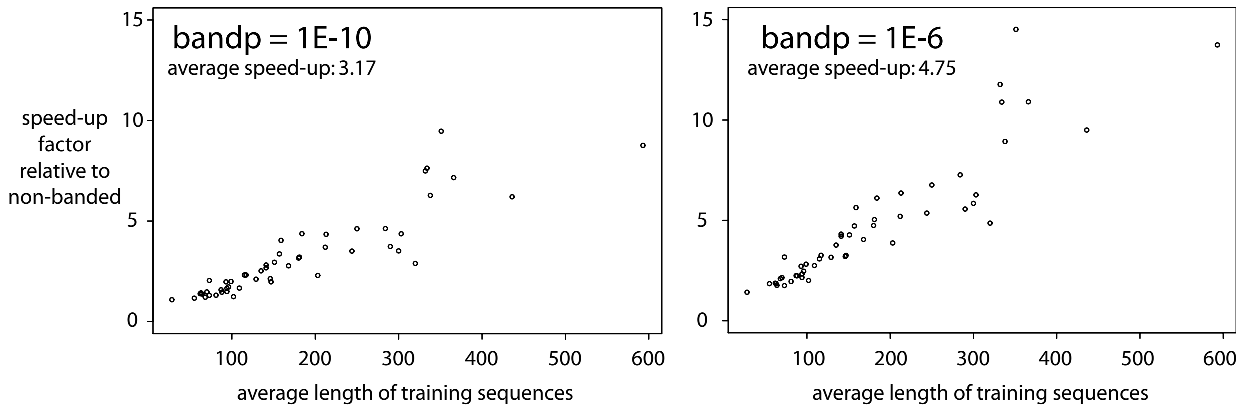

Figure 4: **Acceleration for banded searches of the 51 benchmark families.** Bands calculated with $bandp = 10^{-10}$ (probability mass within each band is 99.99999999%) for left plot and $bandp = 10^{-6}$ (probability mass within each band is 99.9999%) for right plot. There are 51 points in each plot, one for each family in the benchmark set, representing the speed-up for a banded search relative to a non-banded search for the corresponding family.

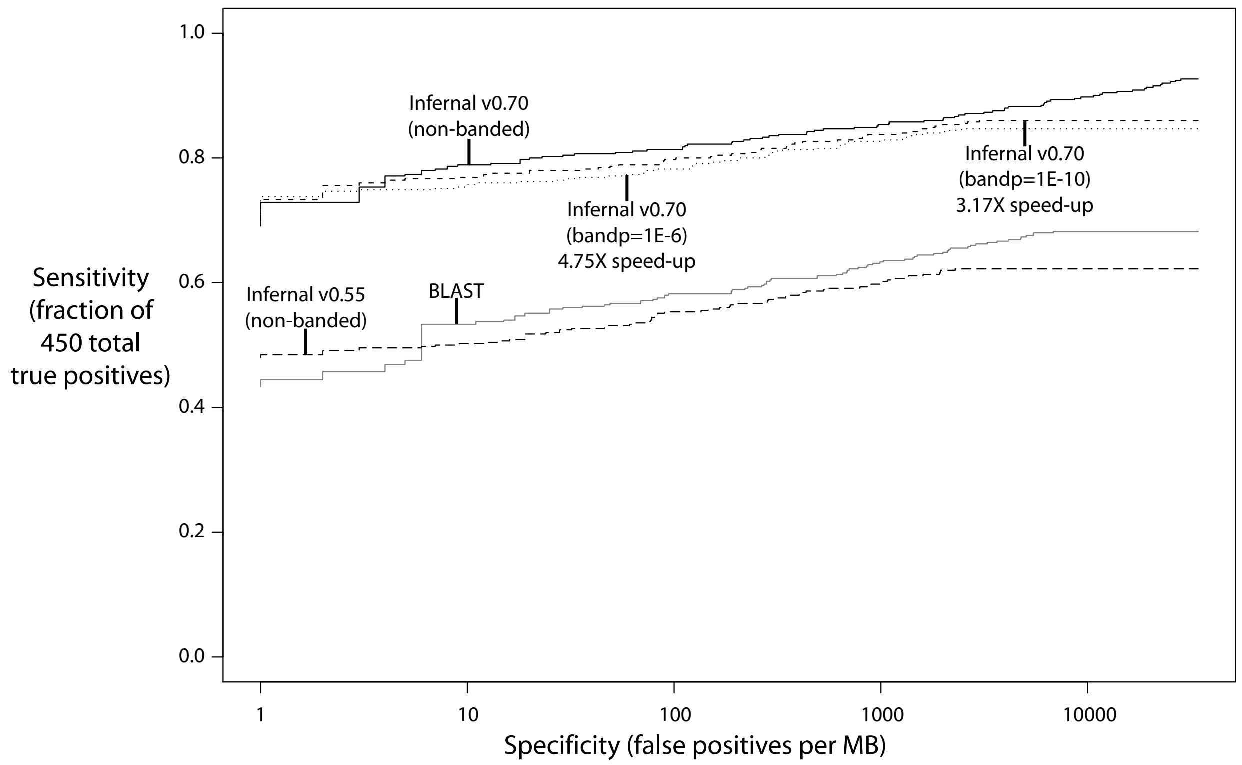

Figure 5: **ROC curve for the Rfam based benchmark.** BLAST : corresponds with row 1 of Table 5; version and options used: `WU-BLASTN-2.0MP --kap -W=7`. INFERNAL v0.55 (non-banded): corresponds with row 2 of Table 5. INFERNAL v0.70 (non-banded): corresponds with row 4 of Table 5. INFERNAL v0.70 ($bandp = 10^{-6}$): corresponds with row 5 of Table 5. INFERNAL v0.70 ($bandp = 10^{-10}$): corresponds with row 6 of Table 5. Speed-up statistics for banded runs are averages over the 51 Rfam benchmark families.